ISSN: 2476-6909; ECOPERSIA. 2020;8(2):77-87

Land Subsidence Modelling Using Particle Swarm Optimization Algorithm and Differential Interferometry Synthetic Aperture Radar

ARTICLE INFO

Article Type
Original Research

Authors
Chatrsimab Z.[1] *MSc,*
Alesheikh A.*[2] *PhD,*
Vosoghi B.[3] *PhD,*
Behzadi S.[4] *PhD,*
Modiri M.[5] *PhD*

How to cite this article
Chatrsimab Z, Alesheikh A, Vosoghi B, Behzadi S, Modiri M. Land Subsidence Modelling Using Particle Swarm Optimization Algorithm and Differential Interferometry Synthetic Aperture Radar. ECOPERSIA. 2020-;8(2):77-87.

ABSTRACT

Aims Land subsidence is one of the phenomena that has been abundantly observed in Iran's fertile plains in recent decades. If it is not properly managed, it will cause irreparable damages. So, regarding the frequency of subsidence phenomenon, the evaluation of the potential of the country's fertile plains is necessary. Towards this, the present study is formulated to assess the vulnerability of the Tehran-Karaj-Shahriyar Aquifer to land subsidence.

Materials & Methods The vulnerability of Tehran-Karaj-Shahriyar Aquifer was determined using the GARDLIF method in a Geographic Information System (GIS) environment. Seven parameters affecting ground subsidence including groundwater loss, aquifer media, recharge, discharge, land use, aquifer layer thickness, and the fault distance were used to identify areas susceptible to land subsidence. Then, they were ranked and weighted in seven separate layers. In the next step, the subsidence location and rates were obtained using the differential interferometric synthetic aperture radar (DInSAR) method. The weights of the input parameters of the GARDLIF model using the subsidence map obtained from the DInSAR method and the particle optimization algorithm (PSO) were then optimized. Accordingly, the subsidence susceptibility map was generated based on the new weights.

Findings & Conclusion The results showed that by increasing correlation coefficient (r) from 0.55 to 0.67 and the amounts of Coefficient of Determination (R^2) from 0.39 to 0.53 between the subsidence index and the obtained subsidence in the aquifer, the optimization of weights applied by the PSO algorithm is more capable for evaluating the land subsidence than the map created by GARDLIF. It was also found that the central parts of the study aquifer had the largest potential for land subsidence.

Keywords DInSAR; GARDLIF; PSO; Subsidence; Vulnerability

[1]Department of GIS/RS, Science and Research Branch, Islamic Azad University, Tehran, Iran

[2]GIS Engineering Department, K.N. Toosi University of Technology, Tehran, Iran

[3]Geodesy Department, K.N. Toosi University of Technology, Tehran, Iran

[4]Civil Engineering Department, Shahid Rajaee Teacher Training University, Tehran, Iran

[5]Geography Urban Panning Department, Malek Ashtar University of Technology, Tehran, Iran

Correspondence
Address: No. 1346, ValiAsr Avenue., Mirdamad Street, Tehran, Iran. Postal Code: 1996715433
Phone: +98 (21) 88786212
Fax: +98 (21) 88786213
alesheikh@kntu.ac.ir

Article History
Received: August 10, 2019
Accepted: December 08, 2019
ePublished: May 19, 2020

CITATION LINKS

[1] Assessment of climate change impacts on groundwater recharge for different soil ... [2] Spatial and temporal analysis of monthly stream flow deficit intensity in ... [3] Land subsidence in Iran caused by widespread ... [4] Assessment of citrus water footprint components ... [5] Assessment of hydro-meteorological drought ... [6] Characteristics and trends of land subsidence in ... [7] Groundwater ... [8] Spatial prediction models for shallow ... [9] Detection of land subsidence in Semarang ... [10] Modeling alluvial aquifer using PMWIN ... [11] Watershed health characterization using reliability-resilience-vulnerability conceptual framework based on hydrological ... [12] Detection of land subsidence in Kathmandu ... [13] Land subsidence: What is it and why is it ... [14] Prediction of ground subsidence in Samcheok City... [15] Assessment of ground subsidence using GIS and ... [16] Land subsidence risk assessment case ... [17] Investigation into subsidence hazards due to ... [18] Assess the potential of land subsidence ... [19] Introducing a new framework for mapping ... [20] Comparison of vulnerability of the southwest Tehran ... [21] Optimization of the ALPRIFT method using a support ... [22] A new approach to determine probable ... [23] Groundwater ... [24] Review: Regional land subsidence accompanying ... [25] Delimitation of ground failure zones due ... [26] Principles of applied ... [27] Groundwater vulnerability map ... [28] Enviromental ... [29] Particle swarm ... [30] Application of fuzzy particle swarm optimization ... [31] Optimization of water allocation during ... [32] Path planning for a planar hyper-redundant manipulator ... [33] Modeling and optimizing lapping process ... [34] A hybrid artificial neural network and ... [35] Topographic mapping from interferometric ... [36] Detection of land subsidence due to excessive ... [37] Dinsar-Based detection of land subsidence and ... [38] Land subsidence modelling using tree-based machine learning ... [39] Tehran-Shahriar Plain subsidence due to excess extraction of underground ... [40] Monitoring its land subsidence and its relation to groundwater harvesting ...

Introduction

Groundwater resources are one of the most important sources of water supply [1] for agriculture, industry and, drinking in many regions of Iran, especially in the central, eastern and southern regions [2, 3], which led to over-exploitation of groundwater from aquifers [4]. Thus, the major problems associated with the inappropriate extraction of underground aquifers water are the persistent groundwater level declination and the sediments and layers accumulation in aquifers [5], which may lead to land subsidence. Land subsidence is one of the environmental problems and geological hazards that has been reported in more than 150 cities of the world [6]. This phenomenon is derived from the natural (including volcanoes, continental drift, acquisition of solutes through rainfall, and so on) and man-made (such as coal and metal mining, and soil salts solution through irrigation, over extraction of groundwater, oil or gas, and also excess construction) reasons [7, 8]. Generally, land subsidence rate occurred due to natural factors is less than one centimeter per year, compared with the man-made factors which reach 50cm per year [9].

The land subsidence, which has been observed in many parts of the world, especially in many plains of Iran, led to endanger human lives and result in heavy financial burdens [10, 11]. This causes topography deformation, damage to urban infrastructure and facilities, severe flooding, and a decrease in the capacity of groundwater aquifers to store water [12]. Therefore, identification of effective factors, modelling, and mapping of the potential land subsidence is very important for preventing such damages [13]. Kim *et al*. [14] using an artificial neural network and geospatial information system, predicted the land subsidence in Samcheok of Korea. They presented the hazard map for land subsidence with 96% validation of field data and subsidence locations in the area. Oh and Lee [15] have been investigated land subsidence by Geographic Information System (GIS) and the Weights-Of-Evidence (WOE) model using seven main factors and reported a high accuracy rate between the subsidence map and the former land subsidence positions. The risk mapping of subsidence using five parameters including land slope, elevation, lithology, distance from the valley-shaped region (sinkholes) and land-use, has obtained by Putra *et al*. [16]. The results indicated that the highest risk areas in accordance with field information observed near the sinkholes region. In order to prepare a potential subsidence map, Xu *et al*. [17] compared the Cosserat continuum model with the Cauchy continuum classic model.

Afifi [18] used Lamb-Whitman experimental relation to evaluate the potential of land subsidence and its effective parameters in the Seyedan-Farooq Plain of Iran. The results showed that the density and compression among clay layers and the inappropriate extraction of underground aquifers were the most effective factors occurring land subsidence. Nadiri *et al*. [19] and Manafiazar *et al*. [20] were estimated the potential of aquifer subsidence using the genetic algorithm and the result verified by subsidence obtained from satellite imagery. The results demonstrated that using the genetic algorithm led to increase the correlation coefficient between the subsidence index and calculated subsidence in the plain. Manafiazar *et al*. [21] also used the ALPRIFT method and support-vector machine (SVM) to evaluate the subsidence vulnerability of southwestern plain of Tehran. The coefficients of the ALPRIFT model improved by the SVM model. The results depicted better efficiency of the SVM model for evaluating the subsidence vulnerability.

In the present study, a vulnerability map of aquifer subsidence has been developed using a new GARDLIF method, provided by Naderi *et al*. [22]. In the next step, the particle swarm optimization (PSO) algorithm was used to optimize the coefficients and results of the GARDLIF method in Tehran-Karaj-Shahriyar Aquifer. The simultaneous using satellite and terrestrial data is the other advantage of this study, which provides the most available and reliable data. In overall, the current study aimed to evaluate the efficiency of the PSO algorithm in improving the coefficients of parameters affecting subsidence susceptibility map as well as to determine the most important parameters in occurrence of this phenomenon for better land management and its control in Tehran-Karaj- Shahriyar Aquifer. Regarding using the PSO algorithm to provide a potential subsidence map, the present study is the first study in this field.

Materials and Methods

Case study

Tehran-Karaj-Shahriyar Aquifer with 5083.97km² width is located in a plain with 2519.8km² width. The study area is located between latitude 35°20′-36°15′ N, and longitude 50°50′-52°15′ E. This aquifer was prohibited by the Ministry of Energy of Iran since 2008 due to the inappropriate extraction of underground water. The maximum and minimum altitude in the study area was 4375 and 800m, respectively. The average temperature and rainfall at altitudes were respectively 11.4°C and 432.5mm/year, and the average temperature and rainfall at the plain were 16.2°C and 227.5mm/year, respectively (Figure 1).

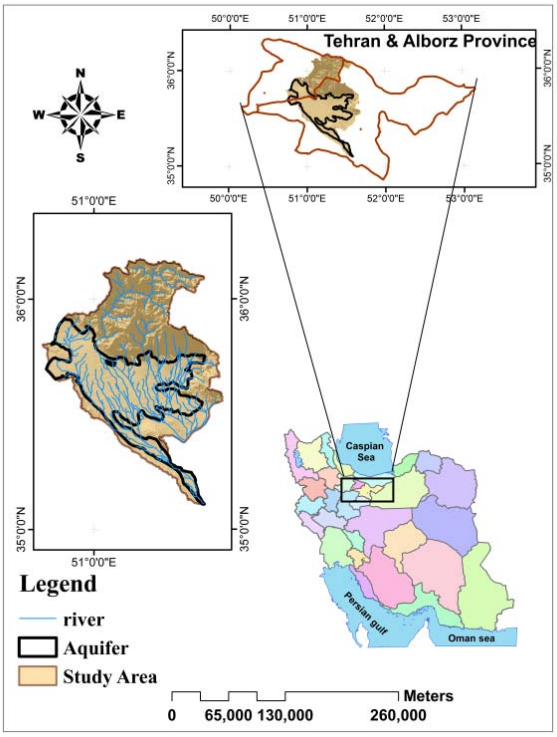

Figure 1) Location of Tehran-Karaj-Shahriyar Aquifer, Iran

According to the last census of groundwater resources in 2011, 40275 wells with an annual discharge of 1931.74 million m³, 1336 springs with an annual discharge of 108.45 million m³ and 429 Qantas with an annual discharge of 226.23 million m³, respectively, have been reported. Water consumption in this area includes 2024.6 million m³ of groundwater (wells and Qantas) and 1013.9 million m³ of surface flows and spring, which 1394.17m³ for agricultural, 1587.41 million m³ for drinking and 65872m³ for industry consumptions have been used.

Growth in groundwater resource utilization was relatively low in the 1950s and 1960s, and then aquifer utilization rates increased from year 1970 onwards. The highest growth rate for aquifer exploitation related to 1999 to 2001 years, with an average growth rate of about 5 million m³/year. Furthermore, according to the statistics and information of piezometric wells from October 1999 to 2015, the amount of changes in groundwater level was between zero to -40m. Consequently, the alluvial aquifer of Tehran-Shahriyar and Karaj plains has fallen by 0.52m on average.

Research methodology

The modelling of potential subsidence of Tehran-Karaj-Shahriyar Aquifer was done using point count system models, GARDLIF, particle swarm optimization algorithm (PSO) and differential interferometric synthetic aperture radar (DInSAR; Figure 2).

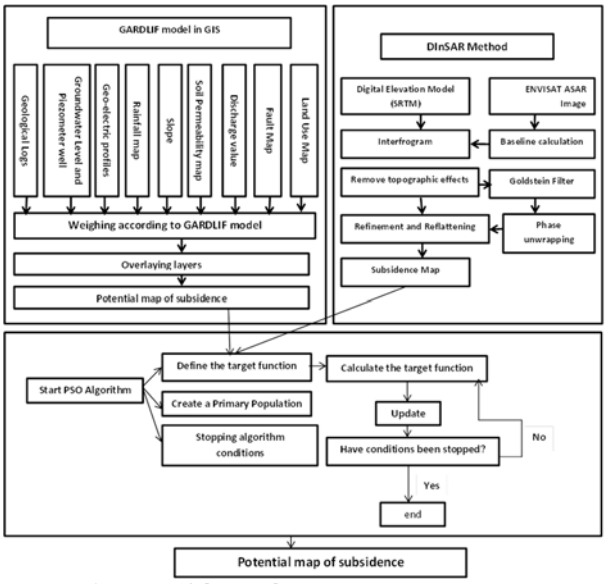

Figure 2) Steps of the study

At the first, the GIS technique has provided layers of effective subsidence parameters including groundwater declination (G), aquifer media (A), net recharge (R), discharge (D), land use (L), impact of aquifer thickness (I), and distance of fault (F) for the GARDLIF model.

Regarding these methods, each effective subsidence parameter has weighed 1-5 and the sub-classes of each parameter were assigned a weight of between 1-10 (Table 1) according to their importance (Equation 1).

(1) SPI= WGr+WAr+WRr+WPr+WLr+WTr+WFr

Table 1) Weights of affecting parameters and rank of each subclass in the GARDLIF model [19, 20, 21]

Subsidence vulnerability indices		Dicline of water table (W=5)		Fault distance (W=1)		Impacts of aquifer thickness (W=2)		Recharge (W=4)		Pumping (W=4)		Land use (W=3)		Aquifer media (W=5)	
Class		Rate	Range (m/y)	Rate	Range (km)	Rate	Range	Rate	Range (cm/y)	Rate	Range (cm/y)	Rate	Range	Rate	Range
Low	24-78	1	0-0.2	10	0-1	1	0-25	10	0-4	1	<0.0001	9-10	Mine	10	Clay
Moderate	78-132	2	0.2-0.5	8	1-2	2	25-55	9	4-9	2	0.0001-0.005	7-9	Agriculture	9	Clay+Silt
High	132-186	3	0.5-0.9	6	2-3	3	55-90	7	9-14	3	0.005-0.01	6-9	Dam site	8	Clay+Sand
Very High	186-240	4	0.9-1.4	4	3-4	4	90-130	5	14-19	4	0.01-0.5	3-8	Residential	3-5	Silt-Clay+Sand
		5	1.4-2	2	4-5	5	130-175	3	19-24	5	0.5-1	3-4	Transportation	4	Sand
		6	2-2.7	1	>5	6	175-225	1	>24	6	1-5	1-3	Dry areas	3	Gravel
		7	2.7-3.5			7	225-280			7	5-20	1	Wasteland	8-10	Organic soils
		8	3.5-4.4			8	280-340			8	20-40	1	Grassland	2	Rubble
		9	4.4-5.4			9	340-405			9	40-65				
		10	>5.4			10	>405			10	>65				

Where SPI was a subsidence vulnerability index, W' denotes weights and following uppercase acronyms represent the GARDLIF data layers, and subscripts 'r' denotes rates.

Seven layers were created based on the weight of the parameters and the weight of the subclasses of each parameter in the GIS environment. Then, by integrating these layers, a subsidence sensitivity map was obtained by the GARDLIF method.

Next, the existing subsidence map of this aquifer was then prepared using SAR radar images from the ENVISAT sensor and the DInSAR method between time intervals 2003 to 2009. In order to optimize the coefficients of the GARDLIF method, the PSO algorithm was used. The input to the PSO algorithm was the weights given to the parameter affecting the subsidence.

The objective function was to maximize the Pearson correlation coefficient between the subsidence maps available in the study area obtained by the DInSAR method and the subsidence potential index obtained from the GARDLIF model. Finally, based on the optimum weights, a subsidence sensitivity map was prepared and compared with the results of DInSAR.

Parameters of GARDLIF model

Aquifer media

Fine-grained soils (such as silt and clay) are more compact compared with sand and pebbles. After underground water extraction, fine-grained soils are going to undergo an irreversible consolidation and resulting to subsidence due to the lack of elasticity and high consolidation coefficients [23]. Therefore, subsidence occurs more frequently in the area containing thick sedimentary deposits or aquifer located between the clay and silt layers [19]. The geological well logs related to the piezometers in the plain, which obtained from the Geological Survey and Mineral Exploration of Iran (https://gsi.ir/fa), were used to prepare this layer. Totally, 109 well logs were used in this study area (Figure 3).

Land use

Various land uses showed different impacts on subsidence rate. The weighing and raster layers were prepared according to Table 1 instructions as well as depicted in Figure 3.

Discharge

There is a balance between recharge and discharge of groundwater aquifer, but agricultural pumping and urban consumption led to destroy this balance and resulting land subsidence [24]. The most important cause of land subsidence in the sedimentary basins is the accumulation of groundwater aquifers due to the excessive pumping of groundwater resources [25]. The higher amount of groundwater extraction resulted in the lower hydraulic pressure and decrease the space between the seeds, which led to increase the effective tension and increased the density of the layers, so the occurrence of subsidence increases [21]. This layer was provided using the annual extraction rate of wells located on the plain. The Thiessen polygon method was applied to determine the exchange rate of each piezometer and then related layer was prepared (Figure 4).

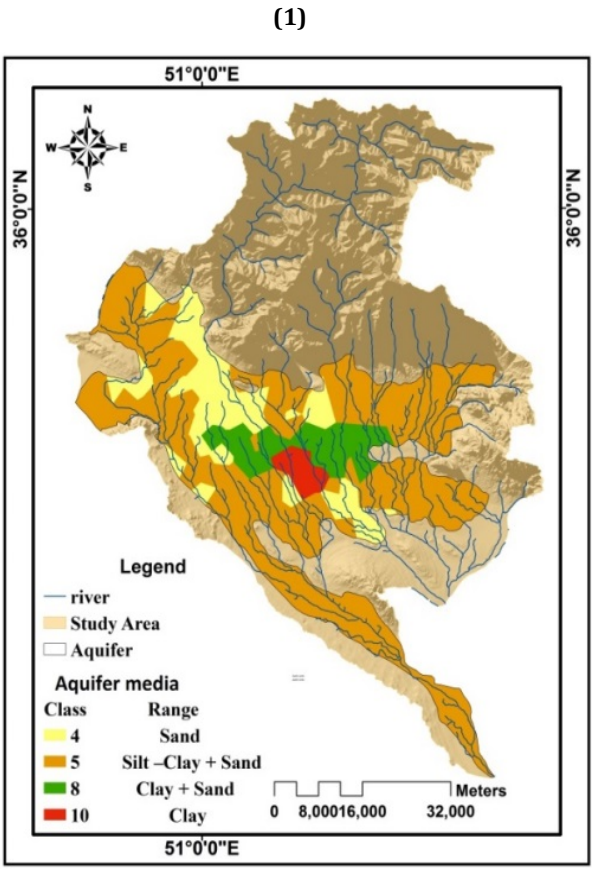

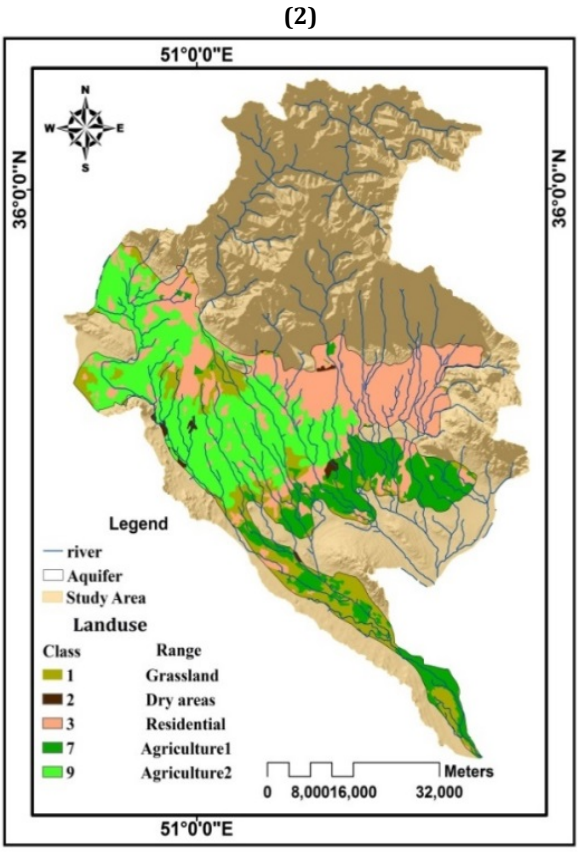

Figure 3) Aquifer media (1) and land use (2) maps of the study area

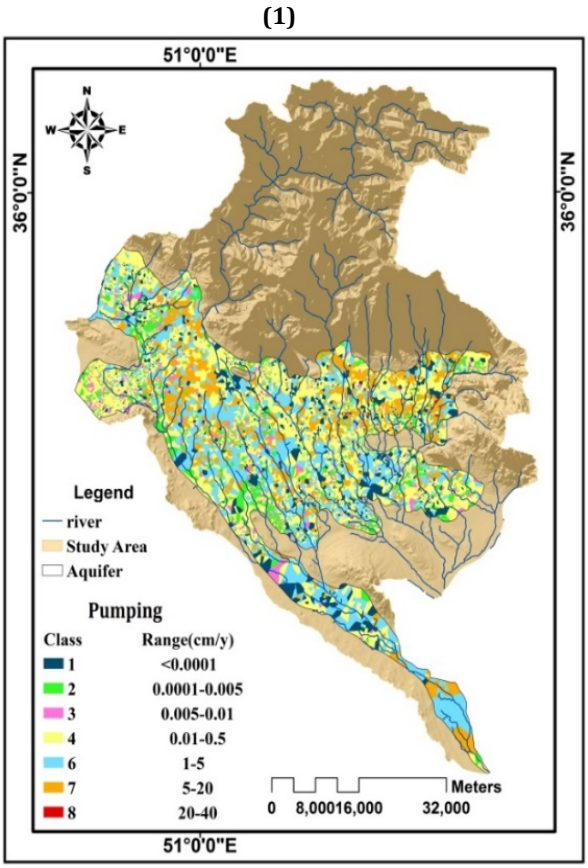

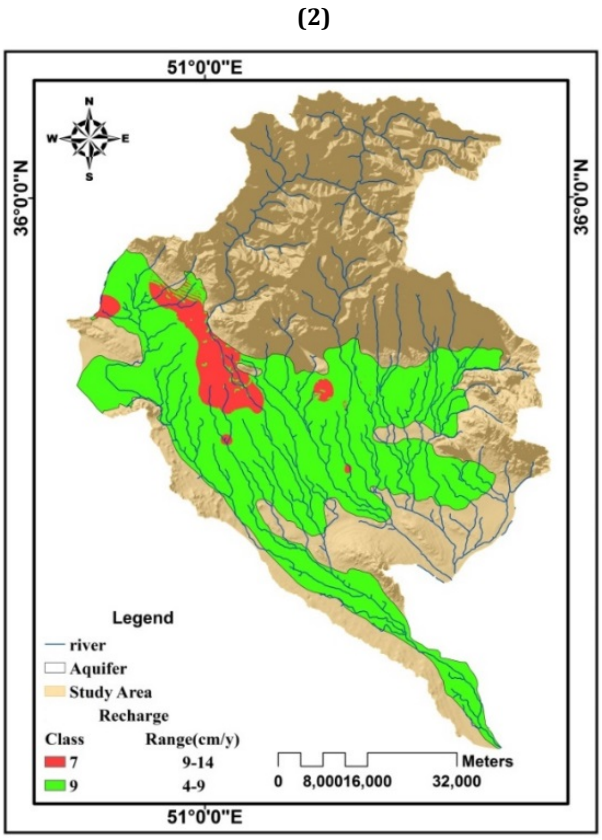

Figure 4) Discharge (1) and recharge (2) rate maps of the study area

Recharge rate

The recharge rate is the amount of water that enters the aquifer from the surface [26]. The higher recharge rate led to increasing the hydraulic pressure and the distance between the seeds, which results in decreasing the effective tension and the occurrence of subsidence. The Piscopo method (2001) [27], which consists of combining of the slope, soil permeability, and rainfall layers, was applied to prepare the layer of recharge rate, then the weighing and raster layers were prepared according to Table 1 (Figure 4).

Aquifer thickness

Areas with high reduction of free surface water and high thickness of the fine-grained and aquifer layers showed greater land subsidence [28]. This layer was prepared using geo-electric sections of the plain, which dates back to 2007. After interpolating and obtaining raster layers, the ranking scale was made according to Table 1 and the final thickness map of the aquifer was obtained (Figure 5).

Distance of fault

GIS Euclidean distance was used to obtain the distance of fault for each point of the plain. Then the resulting map was ranked according to Table 1 (Figure 5).

Groundwater declination

In order to provide this layer, the information of piezometers of the region during seven years was obtained from Tehran Regional Water Authority (http://wrbs.wrm.ir). The difference in water surface was obtained from October 2001 to 2008. After interpolating the whole region data using the Kriging method, the raster layer was obtained to integrate with other layers. This layer was ranked according to Table 1 and eventually, the groundwater declination map was achieved (Figure 6).

Particle Swarm Optimization (PSO) algorithm

This algorithm was proposed by Kennedy and Eberhart in 1995 [29], who used an initial population including potential problem solving to explore the search space. The main idea of the algorithm is that there was the possibility of reaching the goal for each category and all members through their observations and experiences [30]. The responsibility of changing the particles to discover among the solutions by the velocity vector of each particle is one of the differences between this algorithm and the genetic algorithm [31].

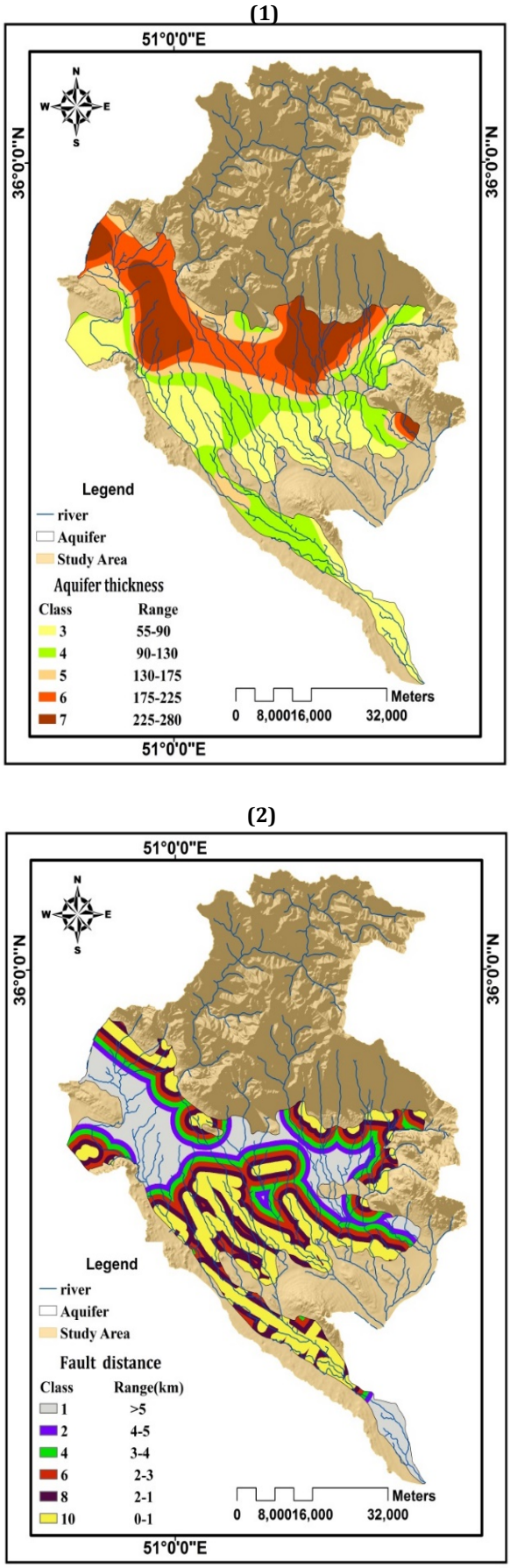

Figure 5) Aquifer thickness (1) and distance of fault maps of the study area (2)

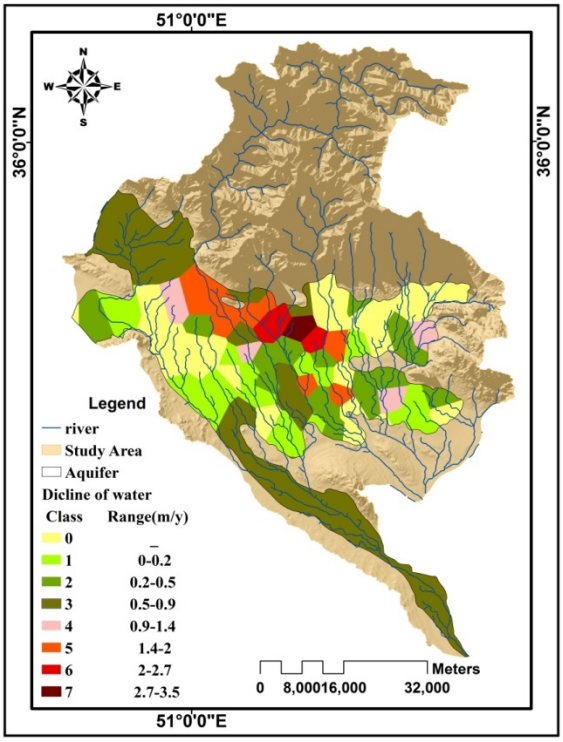

Figure 6) Groundwater declination map of the study area

The particle velocity in each step consists of two parts [32, 33]. The first part was the initial velocity of a particle and the second part was related to the pursuit of the best experience of each particle and with the other particles. The combination of these two parts leads to create a balance in the searches [34]. The Equation 2 was used to update the particle velocity.

(2)

$$V[t+1] = w_i V[t] + C_1 * rand1[t] * (pbest[t] - position[t]) + C_2 * rand2[t] * (gbest[t] - position[t])$$

Which in this equation:
pbest [t]: The best position of each particle at time t
Gbest [t]: The best position for each particle among the whole particles
c1: Constant coefficient (the highest rate of particle motion on the best path)
c2: Constant coefficient of training (motion in the path of the best particle founded in the total population)
rand1 and rand2: Two random numbers with uniform distribution on the interval 0-1
V [t]: Velocity vector at time t
Position [t]: Position vector at time t
The PSO algorithm was used to improve the results and optimize the weights of the parameters affecting subsidence. The input parameters consist of seven weighting parameters affecting the subsidence, which were entered in the model as the initial population. The objective function was to maximize the Pearson correlation coefficient between the subsidences occurring in the area obtained using radar images and the DInSAR method and the subsidence potentials index derived from the integration of the layers (Equation 3).

(3)

$$r = \frac{\sum_{j=1}^{n}(x_j-\bar{x})(y_j-\bar{y})}{\sqrt{\sum_{j=1}^{n}(x_j-\bar{x})}\sqrt{\sum_{j=1}^{n}(y_j-\bar{y})}}$$

Which in this equation:
r: The objective function in the optimization model
n: Number of measured points
xj: Vulnerability index related to point j
$\bar{x}$: Average of vulnerability index
yj: Subsidence rate at point j
$\bar{y}$: Average of subsidence rate
w_i: Weights applied to each Parameter
The condition for stopping this study was similar objective functions in several repetitions. Finally, the GIS technique has provided to map layers using these coefficients and the final map of the subsidence vulnerability generated using this algorithm.

Verification of results using Differential Interferometric Synthetic Aperture Radar (DInSAR) method

The differential interferometric synthetic aperture radar technique was used in this study to examine the subsidence rate. At the first time, this method has been proposed by Goldstein and Zebker [35]. In the DInSAR method, at least three inputs (two SLCs of the area and a DEM digital elevation map) or three SLC images of the area demonstrated the displacement occurs on the land. The accuracy of this method depended on the wavelength of data used which is equal to half of the wavelength (γ/2).
In order to reduce the lack of correlation, the values of the spatial reference and timeline of the images should be considered. The next step is geometric image recording from the same position, which the slave image recorded on the master image. According to the phase difference between the two radar images, the area interferogram was developed using the slave and master image. Until this step, the

geometric error has been eliminated, so in the next step, the topographic error should be removed and appropriate filters should be applied. The SRTM 90-m digital elevation model (DEM) was used in order to eliminate topographic effects [36, 37]. At the final step, the phase correction was applied and the maps of subsidence rate and range were prepared (Figure 7). The ESAR Envisat satellite radar data at C band was used in the present study. The images processing were carried out by SARSCAPE 5.3 software on the ENVI platform.

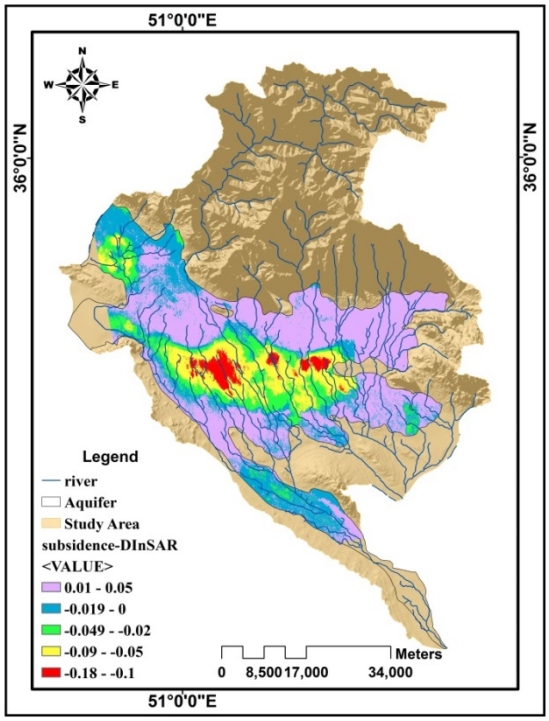

Figure 7) Subsidence map obtained from DInSAR method

Findings and Discussion

The layers were combined based on the weights assigned to each layer in the GARDLIF model and the vulnerability map of the Tehran-Karaj-Shahriyar Aquifer was prepared (Figure 8). The potential subsidence index was estimated in the range from 74 to 188. The PSO model was applied to optimize and evaluate the weights used in the GARDLIF model, which is defined according to the objective function showing the Pearson correlation between the GARDLIF subsidence potential and the radar data subsidence. The weight values of each layer were optimized (Figure 8). Table 2 showed the optimized weights obtained from the PSO algorithm and the weights applied to the GARDLIF model.

Table 2) The weight of parameters affecting subsidence

Model	GARDLIF	PSO
Groundwater declination	5	5
Aquifer media	5	4.6
Recharge rate	4	4.3
Discharge rate	4	3.6
Aquifer thickness	2	2.67
Land use	3	4.1
Distance of fault	1	0.2

(1)

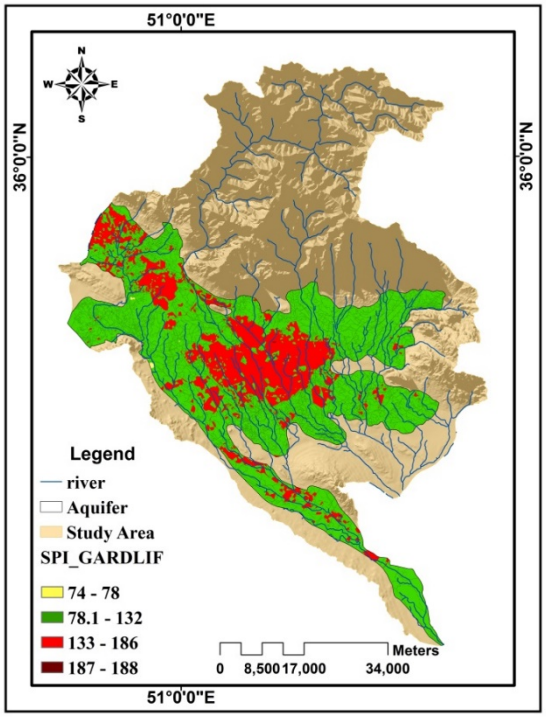

(2)

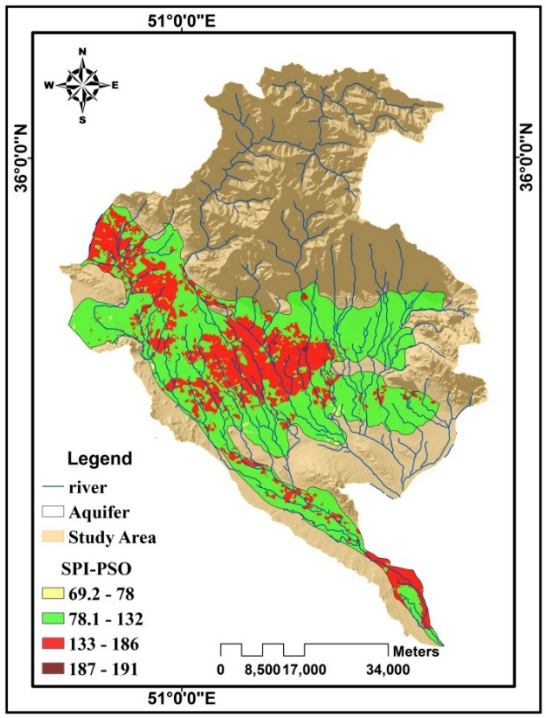

Figure 8) Potential subsidence maps obtained from GARDLIF (1) and PSO (2) methods

Evaluating criteria to assess the accuracy of the models

Correlations index (CI) and the Pearson coefficient were used to compare the used models. In order to use the CI, the subsidence rate was divided into four categories including very high, high, medium, and low [19, 20, 38]. Then, the numbers of wells that demonstrated equal subsidence rate in comparing with the subsidence vulnerability maps and also located in the same group were multiplied by 4. The number of wells which showed the difference of 3, 2, and 1 values subsidence rate than the subsidence vulnerability maps were multiplied by 3, 2, and 1, respectively. Then, the sum values and the correlation index were obtained. The result showed the good correlation between the occurrence of subsidence rate in the study area and the used models.

70 piezometric wells were used in the present study. After that, the subsidence rate obtained by the satellite map was also divided into four categories including very high, high, medium, and low. Table 3 showed the conformance of piezometers and vulnerability groups obtained by the proposed framework and the PSO algorithm. The conformance results demonstrated that the PSO model showed better results with weight optimization than the GARDLIF model. The final results presented in Table 3 and Diagram 1.

Based on the results, the highest subsidence rate according to both methods and differential interferometric map of subsidence occurred in the central part of the plain. Regarding the effect of groundwater declination on subsidence rate, the obtained results showed that the highest groundwater declination has been recorded in the central area of the plain. In line with the obtained results, Razmgir *et al.* [39] also stated that the amount of subsidence in different parts of Tehran-Shahriyar Plain is different and has a V pattern with a maximum subsidence rate of about 16cm per 0.78m of water table fall in the central part. Over-watering was reported as the most important cause of subsidence in the study area. Saffari *et al.* [40] reported the maximum average annual subsidence of 136mm in the period 2003-2010 in the center of Shahriyar Plain where metropolitan area, its gardens and farmland are located. The main cause of the subsidence was related to the indiscriminate extraction of groundwater. In the plain area of the Tehran-Karaj-Shahriyar Aquifer, the size of the sediments was reduced towards the center, so that clay deposits showed a significant effect on the occurrence of subsidence in this section of plain. On the other hand, there are coarse-grained sediments in the northern and southern parts of the plain which played an important role in the recharge rate and water entrance in the aquifer. A wide area of the study plain has been used for agricultural purposes, which based on the inappropriate extraction of underground aquifers water for irrigation showed an important role in subsidence rate. The stated expressions have complied with areas of the high potential of subsidence (Figure 8).

Table 3) Comparison of accuracy criteria of GARDLIF and PSO models

SPI Scores	Very low	Low	Moderate	CI	r	R^2
PSO Model						
Very low	1					
Low	25	18	2	238	0.67	0.536
Moderate		7	15			
GARDLIF Model						
Low	26	19	7	233	0.55	0.395
Moderate		6	10			

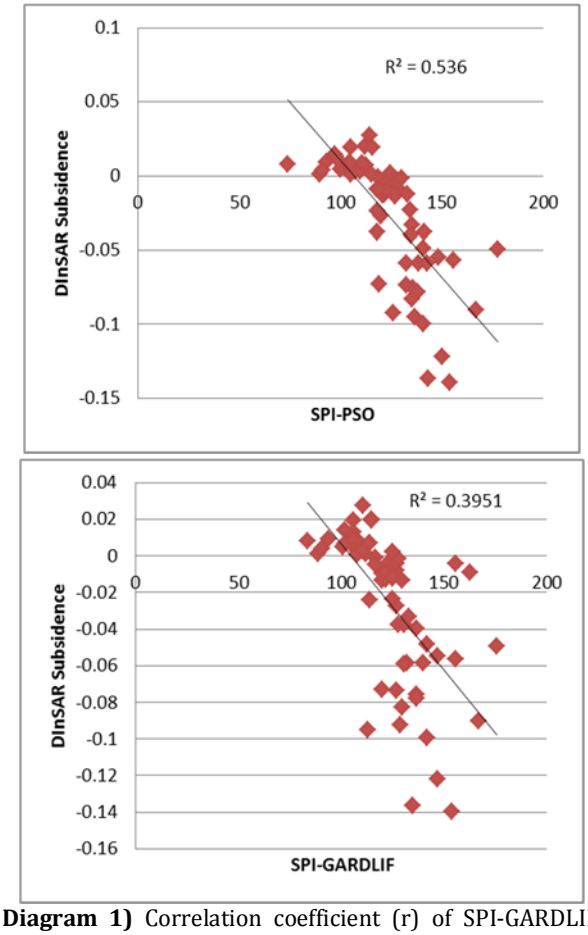

Diagram 1) Correlation coefficient (r) of SPI-GARDLIF, SPI-PSO and DInSAR subsidence rate

Conclusion

Tehran-Karaj-Shahriyar Aquifer is located in Tehran, Shahriyar, Karaj and Fashafuye plains. Increasing population and demand for various water uses led to increase extraction of underground aquifers water during the past two decades, which resulted in a sharp decline in water surface and aquifer volume. Undoubtedly, the continuations of these conditions will cause irreparable consequences. Therefore, the study and assessment of the potential of subsidence are essential in order to manage the destructive effects of land subsidence. Towards this, in the present study, seven parameters affecting subsidence were used in the GARDLIF model. Then, the particle swarm algorithm (PSO) was used to optimize the model coefficients. The results of the present study showed that the method of PSO algorithm due to increase the correlation between normalized subsidence rates and normalized subsidence potentials, demonstrated the vulnerability subsidence of the area better than the GARDLIF method. Based on this model, the northern and southern parts of the plain showed a greater risk of subsidence, so management programs should be done to control and protect these areas.

Acknowledgments: This study was supported by Islamic Azad University, Tehran Science and Research Branch, Islamic Republic of Iran. The authors are grateful to En. Mohammad Hossein Ghavimipanah (Sari Agricultural Sciences and Natural Resources University) and Dr. Zeinab Hazbavi (University of Mohaghegh Ardabili), for their assistance in improving the text and anonymous reviewers for their useful comments and reviews.

Ethical Permissions: None declared by the authors.

Conflict of Interests: The authors state that there is no conflict of interest.

Authors' Contribution: Chatrsimab Z. (First author), Introduction author/Methodologist/Original researcher/Data analyst (30%); Alesheikh AA. (Second author), Data analyst (25%). Vosoghi B. (Third author), Introduction author/Methodologist/Data analyst (20%); Behzadi S. (Fourth author), Introduction author/Data analyst/Discussion author (15%); Modiri M. (Fifth author), Methodologist/Assistant researcher (10%)

Funding/Support: The present study was supported by Islamic Azad University, Tehran Science and Research Branch, Islamic Republic of Iran.

References

1- Motiee H, McBean E. Assessment of climate change impacts on groundwater recharge for different soil types-guelph region in grand river Basin, Canada. Ecopersia. 2017;5(2):1731-44.

2- Alijani R, Vafakhah M, Malekian A. Spatial and temporal analysis of monthly stream flow deficit intensity in Gorganroud watershed, Iran. Ecopersia. 2016;4(1):1313-29.

3- Motagh M, Walter TR, Sharifi MA, Fielding E, Schenk A, Anderssohn J, et al. Land subsidence in Iran caused by widespread water reservoir overexploitation. Geophys Res Lett. 2008;35(16):L16403.

4- Bazrafshan O, Zamani H, Etedali HR, Dehghanpir S. Assessment of citrus water footprint components and impact of climatic and non-climatic factors on them. Sci Hortic. 2019;250:344-51.

5- Bazrafshan O, Parandin F, Farokhzadeh B. Assessment of hydro-meteorological drought effects on groundwater resources in Hormozgan region-South of Iran. Ecopersia. 2016;4(4):1569-84.

6- Hu R, Wang S, Lee C, Li M. Characteristics and trends of land subsidence in Tanggu, Tianjin, China. Bull Eng Geol Environ. 2002;61(3):213-25.

7- Bouwer H. Groundwater hydrology. New York: McGraw Hill College; 1978.

8-. Maleki A, Rezaei P. Forecast locations at risk of subsidence plain Kermanshah. Modarres Hum Sci. 2016;20(1):235-51. [Persian]

9- Kuehn F, Albiol D, Cooksley G, Duro J, Granda J, Haas S, et al. Detection of land subsidence in Semarang, Indonesia, using stable points network (SPN) technique. Environ Earth Sci. 2010;60(5):909-21.

10- Taheri Tizro A, Hosseini A, Kamali M. Modeling alluvial aquifer using PMWIN software and evaluation of subsidence phenomenon in Asadabad plain, Hamedan Province, Iran. Nat Environ Hazards. 2018;7(17):121-36. [Persian]

11- Hazbavi Z, Sadeghi SH. Watershed health characterization using reliability-resilience-vulnerability conceptual framework based on hydrological responses. Land Degrad Dev. 2017;28(5):1528-37.

12- Bhattarai R, Alifu H, Maitiniyazi A, Kondoh A. Detection of land subsidence in Kathmandu Valley, Nepal, using DInSAR technique. Land. 2017;6(2):39.

13- Fulton A. Land subsidence: What is it and why is it an important aspects of groundwater management?. Sacramento: California Department of Water Resources; 2006.

14- Kim K, Lee S, Oh HJ. Prediction of ground subsidence in Samcheok City, Korea using artificial neural networks and GIS. Environ Geol. 2009;58(1):61-70.

15- Oh HJ, Lee S. Assessment of ground subsidence using GIS and the weights-of-evidence model. Eng Geol. 2010;115(1-2):36-48.

16- Putra DP, Setianto A, Keokhampui K, Fukuoka H. Land subsidence risk assessment case study: Rongkop, Gunung Kidul, Yogyakarta-Indonesia. The 4th AUN/SEED-Net Regional Conference on Geo-Disaster Mitigation in ASEA, 2011 October 25-26, Thailand. Unknown Publisher city; Unknown Publisher; 2011.

17- Xu YS, Yuan Y, Shen SL, Yin ZY, Wu HN, Ma L. Investigation into subsidence hazards due to groundwater pumping from Aquifer II in Changzhou, China. Nat Hazard. 2015;78(1):281-96.

18- Afifi MA. Assess the potential of land subsidence and its related factors (Case study: Plain Saidan Farouk MARVDASHT). Quant Geomorphol Res. 2017;5(3):121-32. [Persian]
19- Nadiri AA, Taheri Z, Khatibi R, Barzegari G, Dideban Kh. Introducing a new framework for mapping subsidence vulnerability indices (SVIs): ALPRIFT. Sci Total Environ. 2018;628:1043-57.
20- Manafiazar A, Khamehchiyan M, Nadiri A. Comparison of vulnerability of the southwest Tehran plain aquifer with simple weighting model (ALPRIFT Model) and genetic algorithm (GA). Kharazmi J Earth Sci. 2019;4(2):199-212. [Persian]
21- Manafiazar A, Khamechian M, Nadiri A. Optimization of the ALPRIFT method using a support vector machine (SVM) to assess the subsidence Vulnerability of the southwestern plain of Tehran. J Eng Geol. 2018;11(2):1-14.
[Persian]
22- Naderi K, Nadiri AA, Asghari Moghaddam A, Kord M. A new approach to determine probable land subsidence areas (Case study: The Salmas plain aquifer). Iran J Ecohydrol. 2018;5(1):85-97. [Persian]
23- Bouwer H. Groundwater hydrology. Lotfi-Sadigh A, translator. Tabriz: Sahand University of Technology Press; 1995. [Persian].
24- Galloway DL, Burbey TJ. Review: Regional land subsidence accompanying groundwater extraction. Hydrogeol J. 2011;19(8):1459-86.
25- Pacheco J, Arzate J, Rojas E, Arroyo M, Yutsis V, Ochoa G. Delimitation of ground failure zones due to land subsidence using gravity data and finite element modeling in the Queretaro valley, Mexico. Eng Geol. 2006;84(3-4):143-60.
26- Alizadeh A. Principles of applied hydrology. 9th Edition. Mashhad: Imam Reza university Press; 1996. [Persian].
27- Piscopo G. Groundwater vulnerability map explanatory notes. Parramatta: NSW Department of Land and Water Conservation; 2001.
28- Hafezimoghadas N, Ghafoori M. Enviromental Geology. 1st Edition. Shahrood: Shahrood University of Technology Press; 2009. [Persian].
29- Kennedy J, Eberhart RC. Particle swarm optimization. Proceedings of ICNN'95-International Conference on Neural Networks, 1995 27 November-1 December, Perth, Australia. Piscataway: IEEE; 1995.
30- Enshaee A, Hooshmand R. Application of fuzzy particle swarm optimization in detection and classification of single and combined power quality disturbances. Modares J Electric Eng. 2010;10(2):1-16. [Persian]
31- Moghaddasi M, Morid S, Araghinejad Sh. Optimization of water allocation during water scarcity condition using non-linear programming, genetic algorithm and particle swarm optimization (case study). J Water Res Agric. 2009;4(3):1-13. [Persian]
32- Taherifar A, Alasty A, Salarieh H, Boroushaki M. Path planning for a planar hyper-redundant manipulator with lockable joints using particle swarm optimization. Modares Mech Eng. 2011;11(2):159-75. [Persian]
33- Shafiei Alavijeh M, Amirabadi H. Modeling and optimizing lapping process of 440C steel by neural network and multi-objective particle swarm optimization algorithm. Modares Mech Eng. 2017;17(8):201-12. [Persian]
34- Alizamir M, Azhdary Moghadam M, Hashemi Monfared A, Shamsipour A. A hybrid artificial neural network and particle swarm optimization algorithm for statistical downscaling of precipitation in arid region. Ecopersia. 2017;5(4):1991-2006.
35- Zebker HA, Goldstein RM. Topographic mapping from interferometric synthetic aperture radar observations. J Geophys Res. 1986;91(B5):4993-9.
36- Ahmad W, Choi M, Kim S, Kim D. Detection of land subsidence due to excessive groundwater use varying with different land cover types in Quetta valley, Pakistan using ESA-sentinel satellite data. Nat Hazards Earth Syst Sci Discusss. 2017;1-21.
37- Caló F, Notti D, Galve JP, Abdikan S, Görüm T, Pepe A, et al. Dinsar-Based detection of land subsidence and correlation with groundwater depletion in Konya Plain, Turkey. Remote Sens. 2017;9(1):83.
38- Rahmati O, Falah F, Naghibi SA, Biggs T, Soltani M, Deo RC, et al. Land subsidence modelling using tree-based machine learning algorithms. Sci Total Environ. 2019;672:239-52.
39- Razmgir R, Mousavi M, Shemshaki A, Bolourchi MJ. Tehran-Shahriar Plain subsidence due to excess extraction of underground water, preliminary survey. 1st National Conference on Coastal Water Resources Management, 2010 December 8, Sari, Iran. Sari: Sari University of Agricultural Sciences and Natural Resources; 2010. [Persian]
40- Safari A, Jafari F, Tavakoli Sabour S. Monitoring its land subsidence and its relation to groundwater harvesting case study: Karaj plain-Shahriar. Quant Geomorphol Res. 2016;5(2):82-93. [Persian]